

Accurate Dynamic FIM Estimation from List-Mode PET Data for Uniform Resolution Reconstructions¹

Evren Asma and Richard M. Leahy

Signal and Image Processing Institute, Univ. of Southern California, Los Angeles, CA 90089

Abstract

The Fisher Information Matrix (FIM) plays a key role in the analysis and application of statistical list-mode image reconstruction methods based on inhomogeneous Poisson process data models. The dynamic PET FIM is derived by viewing list-mode data as the limiting case of bin-mode data as the bin-widths approach zero. The Generalized Error Lookup Table (GELT) method developed for the estimation of the FIM from static PET data is extended to estimate the dynamic PET FIM from list-mode data. GELT is a data plug-in technique for estimating reciprocals of mean counts at detector pairs and trades off variance to provide low bias reciprocal mean estimates that are in turn used to compute the FIM. GELT provides accurate FIM estimates even for low count datasets and is therefore particularly suitable for FIM estimation from list-mode data since most spatiotemporal data bins contain only a few counts. As an application, we present simulation results in which the diagonal entries of the dynamic FIM are used to modulate the spatiotemporal smoothing to achieve approximately uniform spatial resolution that remains constant over time.

I. INTRODUCTION

Although mean, variance and resolution properties of static PET image reconstruction methods have been well investigated (cf. [3], [11]), there has been relatively little previous work on the properties of list-mode dynamic PET image reconstruction techniques. In recent work, we developed computationally efficient approximations to the mean and covariance of list-mode dynamic PET reconstructions and also investigated their resolution properties [5, 6]. The application of these techniques to experimental data requires that we estimate the FIM from the observed list-mode data. Here we build on our previous work on the accurate estimation of the static PET FIM and present a technique for estimating the dynamic FIM directly from list-mode data. We then apply this plug-in estimator to the problem of achieving approximately uniform spatial and temporal resolution in dynamic PET.

When dynamic PET images are reconstructed as a series of static PET images, using quadratically penalized maximum likelihood, their resolution properties can vary both from frame to frame and also within a single frame. Spatial variations in resolution for each frame can be significantly reduced using the smoothing methods proposed in [3, 12]. By applying the same

procedure to each frame we can also maintain approximately constant resolution over time. Similarly, when dynamic PET images are reconstructed directly from list-mode data with spatially and temporally invariant smoothing parameters, they may have resolution properties that vary among different regions of interest and over time at a given region of interest. This situation is often undesirable and can potentially lead to large errors in quantitative analyses and make qualitative analysis more difficult. Such variations in resolution can be largely overcome by using a uniform set of temporal basis functions and applying spatiotemporally varying smoothing based on accurate estimates of the diagonal entries of the dynamic PET FIM.

II. METHODS AND RESULTS

A. Image Reconstruction

We model the positron emissions in each voxel in the volume as an inhomogeneous Poisson process [1] whose rate function at voxel j is parameterized by a cubic B-spline basis:

$$\eta_j(t) = \sum_{\ell=1}^{n_b} w_{j\ell} B_{\ell}(t) \quad (1)$$

This model leads to the following list-mode log-likelihood for the set of independent events recorded in the list-mode data [1]:

$$L(\mathbf{w}) = \sum_{i=1}^{n_d} \sum_{k=1}^{x_i} \log \left(\sum_{\ell=1}^{n_b} \sum_{j=1}^{n_v} p_{ij} w_{j\ell} B_{\ell}(a_{ik}) \right) - \sum_{i=1}^{n_d} \left(\sum_{\ell=1}^{n_b} \sum_{j=1}^{n_v} p_{ij} w_{j\ell} \int_0^T B_{\ell}(t) dt \right) \quad (2)$$

where p_{ij} denotes the probability that an event generated at voxel j is detected at detector pair i , $B_{\ell}(t)$ is the ℓ^{th} temporal basis function, x_i denotes the number of events detected at detector pair i , and a_{ik} denotes the arrival time of the k^{th} event at detector pair i . We then maximize the following penalized likelihood objective function to estimate \mathbf{w} :

$$\Phi(\mathbf{w}) = \arg \min_{\mathbf{w} \in \{w | \eta_j(t) \geq 0\}} \{-L(\mathbf{w}) + \sigma(\mathbf{w}) + \rho(\mathbf{w}) + \nu(\mathbf{w})\} \quad (3)$$

where $\sigma(\mathbf{w})$ and $\rho(\mathbf{w})$ are quadratic spatial and temporal penalties respectively and $\nu(\mathbf{w})$ encourages non-negativity.

¹This work was supported in part by Grant R01 EB000363 from the National Institute of Biomedical Imaging and Bioengineering. E.A. is currently with General Electric Global Research, Niskayuna, NY 12309

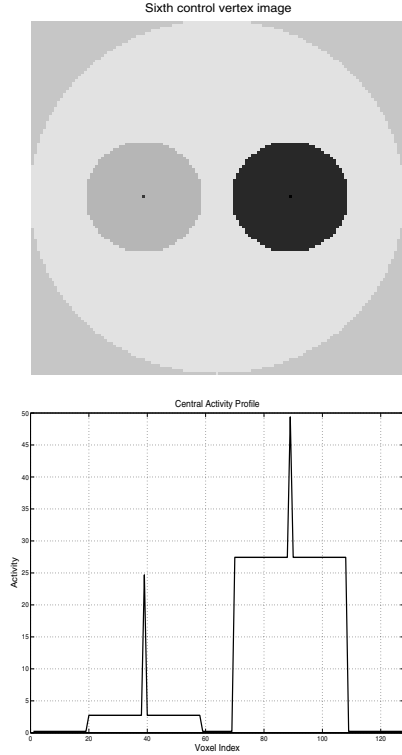


Figure 1: The sixth control vertex image showing the hot and warm cylinders (top) and the associated central profile.

B. Dynamic FIM Estimation

The FIM is not only important in that it provides a bound on the covariance matrix of an unbiased estimator but it also appears in many nuclear medicine applications such as uniform resolution reconstructions [3], error propagation analysis [10], and observer statistic calculations [4]. The ij^{th} element of the FIM matrix \mathbf{F} is given by the following equivalent expressions:

$$\begin{aligned} [\mathbf{F}]_{ij} &= -E \left[\frac{\partial \ln p(\mathbf{y}; \mathbf{x})}{\partial x_i} \frac{\partial \ln p(\mathbf{y}; \mathbf{x})}{\partial x_j} \right] \\ &= -E \left[\frac{\partial^2 \ln p(\mathbf{y}; \mathbf{x})}{\partial^2 x_i x_j} \right] \end{aligned} \quad (4)$$

Applying these definitions using the list-mode log-likelihood to compute the dynamic PET FIM leads to an intractable form because expectations over event arrival times have to be calculated. Since the number of event arrival times at each detector pair is a Poisson random variable under the inhomogeneous Poisson process model, an infinite number of multidimensional integrals have to be evaluated to compute the expectations in (4). Instead, our approach is based on deriving the dynamic FIM by viewing list-mode data as the limiting case of bin-mode data [2] and using accurate reciprocal mean estimation techniques developed for static PET [8] to compute accurate dynamic PET FIM estimates. In this paper, we focus on estimating the *diagonal* entries of the dynamic PET FIM since they will be used in uniform resolution reconstructions.

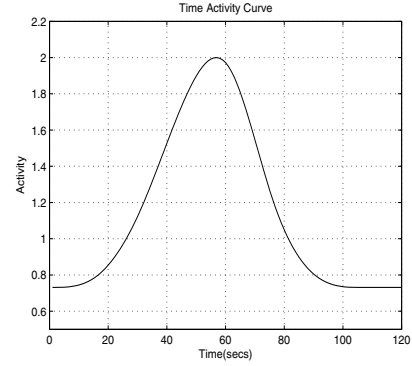


Figure 2: The simulated time activity curve (TAC). The TAC at each voxel was simulated as a scaled version of this curve.

Square roots of the diagonal dynamic FIM entries, $\kappa_{j\ell}$, can be derived using the bin-mode log-likelihood as [2]:

$$\kappa_{j\ell} = \lim_{N \rightarrow \infty} (\mathbf{P} \otimes \mathbf{B})^T \text{diag} \left\{ \frac{1}{y_i^{(n)}} \right\} (\mathbf{P} \otimes \mathbf{B}) \quad (5)$$

$$= \sqrt{\sum_{i=1}^{n_d} p_{ij}^2 \left(\int_0^T \frac{B_\ell^2(t) dt}{r_i(t)} \right)} \quad (6)$$

where \mathbf{P} denotes the system matrix, \mathbf{B} is the temporal sensitivity matrix whose $n\ell^{th}$ element is given by $\int_{t_{n-1}}^{t_n} B_\ell(t) dt$, $B_\ell(t)$ is the ℓ^{th} temporal basis function, \otimes denotes the left Kronecker product, N is the number of time bins that the scan duration is divided into, T is the scan duration and $r_i(t)$ denotes the rate function at detector pair i . Note that while static PET FIM estimates require knowledge of reciprocal means (i.e. $1/\bar{y}_i$) at all detector pairs, dynamic PET FIM estimates require knowledge of *reciprocal rate functions* (i.e. $1/r_i(t)$) at all detector pairs.

In order to use accurate FIM estimation methods developed for static PET [8], we discretize the integral in (6) by partitioning the scan duration in K bins:

$$\kappa_{j\ell} \approx \sqrt{\sum_{i=1}^{n_d} p_{ij}^2 \left(\sum_{k=0}^K \frac{B_\ell^2(t_k) \Delta k^2}{r_i(t_k) \Delta k} \right)} \quad (7)$$

where $K\Delta k = T$ and t_k denotes the midpoint of bin k . Note that the basis functions $B_\ell(t)$ and the bin-width Δk are known exactly. Therefore, we need to estimate the reciprocal mean activity at each bin given by:

$$\frac{1}{r_i(t_k) \Delta k} \approx \frac{1}{\int_{\tau_k}^{\tau_{k+1}} r_i(t) dt} = \frac{1}{\bar{y}_i^k} \quad (8)$$

Equations (7) and (8) convert the estimation of each reciprocal rate function to the problem of estimating K reciprocal means: $\{1/\bar{y}_i^k\}_{k=1}^K$. In medium or high count

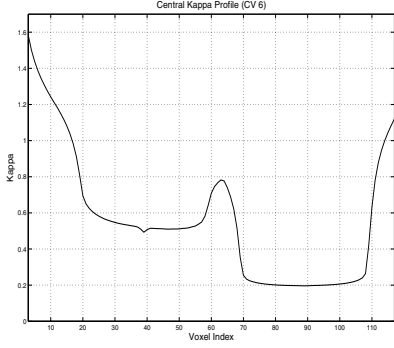


Figure 3: True central κ profile for the sixth control vertex (i.e. temporal basis function). The profile indicates that the smoothing in the hot cylinder should be approximately 3 times less than that in the warm cylinder for resolution uniformity.

situations (i.e. average counts/bin > 5) one can use the “direct plug-in” (DPI) or “modified plug-in” (MPI) methods [8] to estimate reciprocal means:

$$\left[\frac{1}{\bar{y}_i^k} \right]_{DPI} = \frac{1}{y_i^k} \quad \left[\frac{1}{\bar{y}_i^k} \right]_{MPI} = \frac{1}{y_i^k + 1} \quad (9)$$

However, in list-mode reconstructions, an accurate discretization of the integral in (6) requires many time bins with only a few counts per bin and therefore an accurate method to estimate the reciprocal means in low-count situations is necessary. Note that diagonal FIM entries are sensitive to bias in reciprocal mean estimates but are relatively robust to variance because of the weighted averaging with p_{ij}^2 's. Based on this observation, in [8] we presented such a method (Generalized Error Lookup Table, GELT) that trades off variance for low bias in reciprocal mean estimates to provide more accurate FIM estimates.

The GELT reciprocal mean estimates are given by:

$$\left[\frac{1}{\bar{y}_i^k} \right]_{GELT} = \frac{D_{y_i^k}}{y_i^k + 1} \quad (10)$$

where $D_y = C_y$ for $y \leq N$ and $D_y = 1$ for $y > N$ and the C_y terms are estimated as the coefficients that minimize the generalized error $G \equiv B + wV$. Here B denotes bias, V denotes variance and $w \ll 1$ determines their relative weights. The details of GELT estimation are presented in [8] and are not repeated here. Our final estimate for the dynamic PET FIM becomes:

$$\hat{\kappa}_{j\ell} \approx \sqrt{\sum_{i=1}^{n_d} p_{ij}^2 \left(\sum_{k=0}^K B_\ell^2(t_k) \Delta k^2 \left[\frac{1}{\bar{y}_i^k} \right]_{GELT} \right)} \quad (11)$$

In the next section, we compare diagonal dynamic PET FIM entries obtained via DPI, MPI and GELT in a uniform resolution reconstruction application.

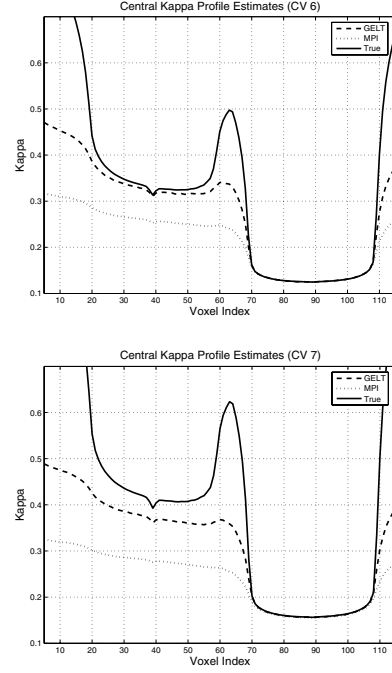


Figure 4: GELT and MPI κ profile estimates shown together with the true profile for control vertices 6 (top) and 7.

C. Uniform Resolution over Space and Time

We approach the resolution problem through the linearized local impulse response (LIR) as in [3] and try to make the linearized LIR to a perturbation of a control vertex spatially uniform and constant over time. Again, we use the bin-mode log-likelihood to compute the linearized LIR and allow the bin-widths to approach zero. The resulting linearized LIR is given by:

$$\mathbf{L}^{j\ell}(\mathbf{w}) = [(\mathbf{P}^T \mathbf{P} \otimes \mathbf{B}^T \mathbf{B}) + \beta \mathbf{D}_\kappa^{-1} \mathbf{R}_S \mathbf{D}_\kappa^{-1} + \gamma \mathbf{D}_\kappa^{-1} \mathbf{R}_T \mathbf{D}_\kappa^{-1}]^{-1} (\mathbf{P}^T \mathbf{P} \otimes \mathbf{B}^T \mathbf{B}) \mathbf{e}_{j\ell} \quad (12)$$

where β and γ are the spatial and temporal smoothing parameters respectively, \mathbf{R}_S and \mathbf{R}_T are the second derivative matrices for the quadratic spatial and temporal penalties respectively, \mathbf{D}_κ is the diagonal matrix whose $(j\ell, j\ell)^{th}$ element is $\kappa_{j\ell}$, and $\mathbf{e}_{j\ell}$ is the unit vector in the $j\ell^{th}$.

Uniform spatial resolution that remains constant over time can be approximately achieved by making the linearized LIR expression shift invariant in j and ℓ and using uniform temporal basis functions. If non-uniform basis functions form a better temporal model, the reconstruction can be performed in a transformed time domain (by warping event arrival times) where uniform basis functions form an accurate model and the rate function estimates can then be warped back to the original time domain [7]. The use of the following spatial and temporal penalties make the linearized LIR shift invariant in j and ℓ up to the approximations in [3] and [6]:

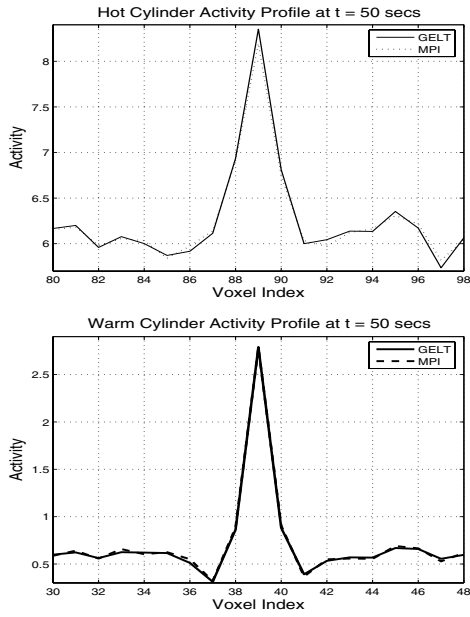


Figure 5: Hot and warm cylinder profiles at $t = 50$ secs for GELT and MPI. Recovered peak ratios between hot and warm cylinders were 0.9950 for GELT compared to 0.9340 for MPI (True ratio = 1).

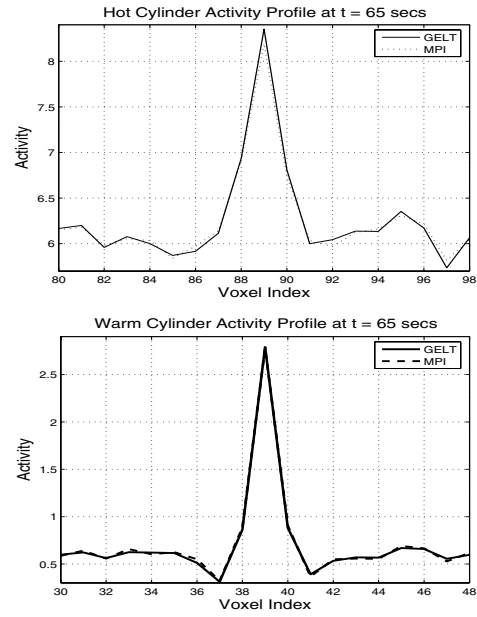


Figure 6: Hot and warm cylinder profiles at $t = 65$ secs for GELT and MPI. Recovered peak ratios between hot and warm cylinders were 1.0099 for GELT compared to 0.9479 for MPI (True ratio = 1)

$$\sigma(\mathbf{w}) = \beta \sum_{\ell=1}^{n_b} \sum_{j=1}^{n_v} \sum_{j' \in \mathcal{N}_j, j' > j} \zeta_{jj'} \hat{\kappa}_{j\ell} \hat{\kappa}_{j'\ell} (w_{j\ell} - w_{j'\ell})^2 \quad (13)$$

$$\rho(\mathbf{w}) = \gamma \sum_{j=1}^{n_v} \sum_{\ell_1=1}^{n_b} \sum_{\ell_2=1}^{n_b} \hat{\kappa}_{j\ell_1} \hat{\kappa}_{j'\ell_2} w_{j\ell_1} Q_{\ell_1\ell_2} w_{j\ell_2} \quad (14)$$

Note that both penalties vary spatiotemporally according to the estimates of the diagonal elements of the dynamic PET FIM, $\hat{\kappa}_{j\ell}$. Therefore accurate estimation of the diagonal FIM entries from real data play a critical role in achieving uniform resolution.

D. Simulations

We estimated the dynamic FIM entries using DPI, MPI and GELT on 150 simulated datasets with 1M counts each over 120 seconds. The datasets were generated from a single-ring ECAT HR+ scanner that contained a hot and a warm cylinder in a very low activity background. Each cylinder had a hot line source at its center (Figure 1). The rate function at each voxel was simulated as the scaled version of a single time activity curve shown in Figure 2 and the HCL:HCB:WCL:WCB:B activity ratios were 20:11:10:1:0.02 making the activity ratio between the hot and warm cylinder backgrounds 11:1 and the additional activity contribution due to the line source constant for both cylinders (HCL: hot cylinder line source, HCB: hot cylinder background, WCL: warm cylinder line source, WCB: warm cylinder background, B:background). This resulted in κ profiles such as the one shown in Figure 3 for the sixth temporal basis function. Images were reconstructed using 30 preconditioned conjugate gradient iterations [9], and 11 uniformly spaced cubic B-splines. The smoothing parameters

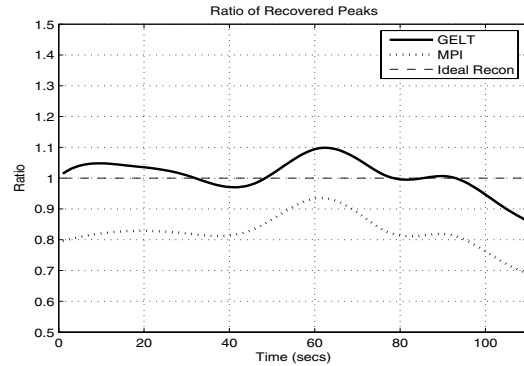


Figure 7: Ratio of the recovered peaks for MPI and GELT. The recovered peak ratio for GELT is close to that of the ideal reconstruction (i.e. 1) whereas MPI recovers approximately 20% less contrast compared to GELT.

were $\beta = 0.005$ and $\gamma = 500$.

Figure 4 shows the estimated diagonal FIM entries for MPI and GELT ($N=5$) together with the true profile for control vertices 6 and 7. FIM estimation results for DPI are not shown here because its performance was significantly reduced due to the large number of empty spatiotemporal bins. We used $K = 40$ uniformly spaced 3-second spatiotemporal bins.

Figures 5 and 6 show the reconstructed central profiles at $t = 50s$ and $t = 65s$ respectively with spatiotemporally varying smoothing using diagonal FIM estimates obtained via MPI and GELT. Note that both reconstructions are designed to achieve uniform resolution and differ only in the manner in which they estimate the FIM to achieve this. When the smoothing parameters are modulated according to the dynamic

FIM estimates obtained with our GELT method, resolution in both cylinders remains approximately uniform as demonstrated by the approximately equal peak to background ratios in both cylinders. Inspection of Figures 5 and 6 indicates only small differences between the results using MPI and GELT, but as shown in Figure 7, when taking the ratio of the recovered peaks between hot and warm cylinders we obtain a value closer to the correct value of unity using GELT than with MPI which exhibits approximately 20% loss in contrast recovery. Here we defined the recovered peak as additional activity at the center of the cylinder due to the line source (i.e. activity at center minus mean background activity) divided by mean background activity.

E. Conclusions

We presented a computationally efficient method for achieving approximately uniform spatial resolution in list-mode dynamic PET reconstructions by using an accurate plug-in estimator for the dynamic PET FIM and compared the performances of our GELT method and MPI. We expect GELT FIM estimation to be useful in many statistical analysis and reconstruction applications that operate directly on list-mode data and require the estimation of the FIM from real data.

III. REFERENCES

- [1] T.E. Nichols, J.Qi, E. Asma, and R.M. Leahy. Spatiotemporal reconstruction of list-mode PET data. *IEEE Transactions on Medical Imaging*, 21(4):396–405, 2002.
- [2] E. Asma, and R.M. Leahy, “Mean and covariance properties of dynamic PET reconstructions from list-mode data.” *IEEE Transactions on Medical Imaging*, in press.
- [3] J. Fessler and W. Rogers, “Spatial resolution properties of penalized-likelihood image reconstruction: space-invariant tomographs,” *IEEE Transactions on Medical Imaging*, 5(9):1346–58, 1996.
- [4] P. Bonetto, J. Qi, and R.M. Leahy, “Covariance approximation for fast and accurate computation of channelized Hotelling observer statistics,” *IEEE Transactions on Nuclear Science*, 47(4):1567–72
- [5] E. Asma, T.E. Nichols, and R.M. Leahy, “Temporal resolution properties of dynamic PET reconstructions,” in *Proc. 2002 IEEE NSS-MIC*, vol. 2, pp.778–81.
- [6] E. Asma, and R.M. Leahy, “Temporally invariant uniform spatial resolution in dynamic PET,” in *Proc. 2003 IEEE NSS-MIC*, vol. 5, pp.3092–96.
- [7] E. Asma, and R.M. Leahy, “Theoretical comparison of uniform resolution penalized likelihood dynamic PET reconstructions with multiframe penalized likelihood static PET reconstructions.” in *Proc. 2004 IEEE NSS-MIC*.
- [8] Q.Li, E.Asma, J.Qi, J.R. Bading, and R.M. Leahy, “Accurate estimation of the Fisher Information Matrix for the PET image reconstruction problem.” *IEEE Transactions on Medical Imaging*, 23(9):1057–64, 2004.
- [9] E. Mumcuoglu, R.M. Leahy, S. Cherry, and Z. Zhou, “Fast gradient based methods for Bayesian reconstruction of transmission and emission PET images,” *IEEE Transactions on Medical Imaging*, 13(4):687–701, 1994.
- [10] J. Qi and R.H. Huesman, “Propagation of errors from the sensitivity image in list mode reconstruction,” *IEEE Transactions on Medical Imaging*, 23(9):1094–99, 2004
- [11] J. Qi and R. Leahy, “Resolution and noise properties of MAP reconstruction for fully 3D PET.” *IEEE Transactions on Medical Imaging*, 19(5):293–305, 2000.
- [12] J. Stayman and J. Fessler, “Compensation for nonuniform resolution using penalized-likelihood reconstruction in space-variant imaging systems.” *IEEE Transactions on Medical Imaging*, 23(3):269–84, 2004.